http://www.jmaterenvironsci.com/

Structure of two new K₂SnX(PO₄)₃ (X = Cr, In) Langbeinite-type phases

A. Aatiq[*], H. Bellefqih, A. Marchoud, R. Fakhreddine, N. Boudar, R. Tigha

Département de Chimie, Laboratoire de Physico-Chimie des Matériaux Appliqués, Université Hassan II de Casablanca, Faculté des Sciences Ben M'Sik, Avenue Idriss El harti, B.P. 7955, Casablanca, Morocco.

Abstract

Structures of two $K_2SnX(PO_4)_3$ (X= Cr, In) phosphates, obtained by conventional solid state reaction techniques at 950 °C, were determined at room temperature from X-ray powder diffraction (XRD) using the Rietveld analysis. The two materials exhibit the Langbeinite-type structure ($P2_13$ space group, Z = 4). Cubic unit cell parameter values are: a = 9.8741(1) Å and a = 10.0460(1) Å for $K_2SnCr(PO_4)_3$ and $K_2SnIn(PO_4)_3$ respectively. Final Rietveld refinements lead to acceptable reliability factors (e.g., R_{wp} = 9.1%; R_B = 5.2% for $K_2SnCr(PO_4)_3$ and R_{wp} = 8.1%; R_B = 5.1% for $K_2SnIn(PO_4)_3$). Langbeinite frameworks are principally built of $Sn(X)O_6$ octahedra sharing corners with PO_4 tetrahedra. Structural refinements show that the two crystallographically independent octahedral sites (of symmetry 3) have a mixed Sn/X (B = Cr, In) population. The two potassium cations occupied large isolated cages within the framework.

1. Introduction

Structures of phosphates with general formula $A_xXX'(PO_4)_3$ typically consist of a $XX'(PO_4)_3$ framework which is built up by corner-sharing $X(X')O_6$ octahedra and PO_4 tetrahedra in such a way that each octahedron is surrounded by six tetrahedra and each tetrahedron is connected to four octahedral. Depending on the size of the A, X, and X' cations and the value of x, the $A_xXX'(PO_4)_3$ compounds can crystallise in Nasicon-type structure, Langbeinite-type or $Sc_2(WO_4)_3$-type [1-3]. One important difference between the two first structures is that in langbeinite the framework creates closed cavities that trap alkali cations, while in Nasicon, A^+ cations are found in the intersection of tunnels through which they can diffuse. All these structures are related to each other by simple distortions and/or rotations of the cationic polyhedra. There are a number of reports on the synthesis and investigation of Langbeinite-related complex phosphates, which exhibit interesting properties such as magnetic luminescence and phase transitions [4-8]. It should be noted that compounds with a langbeinite-type structure are also prospects for use as a matrix for the storage of nuclear waste. Note that it has been proved that cesium can be introduced into the cavity of a Langbeinite framework that can be used for the immobilization of ^{137}Cs in an inert matrix for safe disposal [9,10]. Depending of A and B(B') metal cation charge, approximately five general formula for phosphate with Langbeinite structure are known (i) $A^+B^{4+}_2(PO_4)_3$ (e.g., $KTi_2(PO_4)_3$) (ii) $A^+A^{2+}B^{3+}_2(PO_4)_3$ (e.g., $KBaFe_2(PO_4)_3$), (iii) $A^+_2B^{3+}B'^{4+}(PO_4)_3$ (e.g., $K_2YbTi(PO_4)_3$), (iv) $A^+_2B^{2+}_{0.5}B'^{4+}_{1.5}(PO_4)_3$ (e.g., $K_2Co_{0.5}Ti_{1.5}(PO_4)_3$), and (v) $A^{2+}_{1.5}B^{3+}_2(PO_4)_3$ (e.g., $Pb_{1.5}V_2(PO_4)_3$) [2,11-13]. Recently the structural determination from powder X-ray diffraction of some phosphates tin of Nasicon-type family has been realised in our laboratory [14-16]. In fact, among a great variety of Langbeinite-type based phosphate only few compounds containing tin were reported. Thus, the structure of the two $K_2SnB(PO_4)_3$ (B = Fe, Yb) Langbeinite-type phases have been determined from powder X-ray diffraction by some of us [17] and to our knowledge, only the structural studies of the two $K_2SnAl(PO_4)_3$ and $K_2SnSc(AsO_4)_3$ Langbeinite phases have been reported [18,19]. Herein the principal objective of this study was the synthesis and structural determination of the two tin $K_2SnX^{3+}(PO_4)_3$ (X = Cr, In) compounds.

2. Experimental details

Syntheses of $K_2SnX(PO_4)_3$ (X = Cr, In) were carried out using conventional solid-state reaction techniques. Powder crystalline samples were prepared from mixtures of carbonate K_2CO_3, oxides In_2O_3, Cr_2O_3 and SnO_2 and the phosphate $NH_4H_2PO_4$ in stoichiometric proportions. The mixtures were heated progressively with intermittent grinding at 200 °C (12 h), 600 °C (12 h), 800 °C (16 h) and 950 °C (48 h) in air. The products of

reaction were characterised by XRD at room temperature with a Philips X' Pert MPD (θ-2θ) diffractometer; (CuKα) radiation (40 KV, 40 mA). The data were collected from 10 to 90° (2θ), in steps of 0.02°, with a counting time of 30s per step. The Rietveld refinement of the structure was performed using the Fullprof program [20].

3. Resulats and Discussion

The peak positions and intensities of the two XRD patterns for $K_2SnCr(PO_4)_3$ and $K_2SnIn(PO_4)_3$ (Figure 1) were close to those of Langbeinite-type $K_2SnFe(PO_4)_3$ ($P2_13$ space group, Z = 4) [17]. The cubic cells of both materials were found by Dicvol program [21]. The corresponding figures of merit are (M20/F20 = 146.5/236.9(0.0013, 65) and (F(31) = 48.7(0.0015, 434)) for $K_2SnCr(PO_4)_3$ and (M20/F20 = 206.1/246.7(0.0011, 55) and (F(31) = 53.7(0.0011, 412)) for $K_2SnIn(PO_4)_3$. Obtained parameter values are a = 9.8741(1) Å and a = 10.0460(1) Å for $K_2SnCr(PO_4)_3$ and $K_2SnIn(PO_4)_3$ respectively. The unit cell parameter of $K_2SnIn(PO_4)_3$ is larger than that for $K_2SnCr(PO_4)_3$ because the ionic radius of In^{3+} (r_{In}^{3+} = 0,80 Å) is greater than that of Cr^{3+} (r_{Cr}^{3+} = 0,615 Å) [22]. In fact, the variation of the a-parameter of $K_2SnX(PO_4)_3$ (X = Al, Cr, Fe, In, Yb) series as a function of the ionic radius of the X^{3+} ions shows a gradual increase when the ionic radii (r_X^{3+}) of X^{3+} in six coordination increases. Thus for the $K_2SnX(PO_4)_3$ phases, the a-parameter values were respectively 9.798(1) Å for X = Al (r_{Al}^{3+} = 0,535 Å), 9.921(1) Å for X = Fe (r_{Fe}^{3+} = 0,645 Å), and 10.150(1) Å for X = Yb (r_{Yb}^{3+} = 0,868 Å). In the following discussion, the structural refinements were based upon the above mentioned assumption.
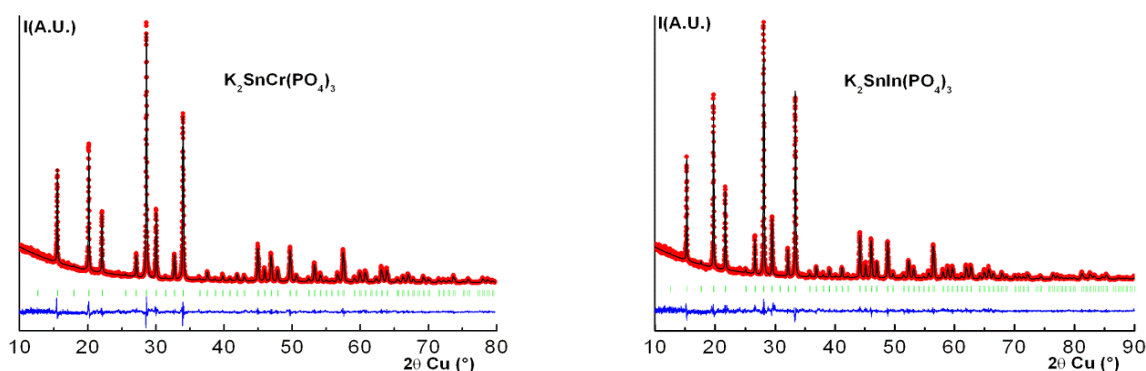
Figure 1: Comparison of the experimental (•••), calculated (—) and difference profile (—) of the XRD pattern of $K_2SnCr(PO_4)_3$ and $K_2SnIn(PO_4)_3$. Vertical bars in green correspond to the allowed Bragg reflections.

3.1. Rietveld refinement of $K_2SnX(PO_4)_3$ (X = Cr, In)

Initial starting parameters for the Rietveld refinement of $K_2SnX(PO_4)_3$ (X = Cr, In) were based on those already reported for $K_2SnFe(PO_4)_3$ Langbeinite-phase [17]. At first, the profile matching refinement was performed then background and scaling factors were added to the refined parameters. On the next stage, the atomic position were refined. The two K atoms in $K_2SnX(PO_4)_3$ were located at the K(1) and K(2) sites (4a positions) of Langbeinite-type $K_2SnFe(PO_4)_3$. The P and O atoms were all located in independent 12b positions. According to previous investigations of Langbeinite related phosphates, in a first step of refinement the Sn and X atoms in $K_2SnX(PO_4)_3$ (X = Cr, In) were distributed respectively in the two different octahedral M1 (~0.58, ~0.58, ~0.58) and M2 (~0.86, ~0.86, ~0.86) sites of Langbeinite-structure. In the final refinements, the occupancies of Sn and Cr atoms in both crystallographically possible M1 and M2 sites of the $K_2SnCr(PO_4)_3$ material were allowed to vary, but the total atomic contents were constrained to be one for Sn and one for Cr atoms per formula unit. The observed, calculated and difference XRD patterns of both $K_2SnX(PO_4)_3$ (X = Cr, In) phases are given in Figure 1, respectively. As shown in Table 1, this last refinement leads to a mixed Sn/Cr population within the two crystallographically independent M1 and M2 octahedral sites. Note that in the case of $K_2SnIn(PO_4)_3$, occupancies of Sn and In atoms were not allowed to vary because XRD data cannot distinguish, without difficulty, between the two isoelectronic Sn^{4+} and In^{3+} cations Table 2.

3.2. Structure description of $K_2SnX(PO_4)_3$ (X = Cr, In) Langbeinite phases

The two Langbeinite $K_2M_2(PO_4)_3$ (M = Sn/Cr, Sn/In) frameworks are built of MO_6 octahedra sharing corners with PO_4 tetrahedra (Figure 2a). A simple description of the framework is based on [$M_2P_3O_{18}$] units composed of two MO_6 octahedra linked together by three PO_4 tetrahedra. Each PO_4 shares two corners with $M(1)O_6$ octahedra and two corners with $M(2)O_6$ octahedra.

Table 1: Results of the Rietveld refinement of $K_2SnCr(PO_4)_3$

K2SnCr(PO4)3						
Space group, $P2_13$; [Z = 4, a = 9.8741(1) Å; V = 963(1) Å^3]						
Pseudo-voigt function, PV = ηL + (1-η)G; η = 0.687(1)						
Half-width parameters, U = 0.093(4), V = -0.010(5), and W = 0.010(2)						
Conventional Rietveld R-factors, R_{WP} = 9.1 %; R_P = 7.0 %; R_B = 5.2 %; R_F = 4.1 %						
Atom	Site	Wyckoff positions			B_{iso}(Å^2)	Occupancy
K(1)	4a	0.0664(7)	0.0664(7)	0.0664(7)	1.8(1)	1
K(2)	4a	0.2921(5)	0.2921(5)	0.2921(5)	1.8(1)	1
M(1) = Sn(1)/Cr(1)	4a	0.5861(3)	0.5861(3)	0.5861(3)	0.7(1)	0.47/0.53(1)
M(2) = Sn(2)/Cr(2)	4a	0.8532(3)	0.8532(3)	0.8532(3)	0.7(1)	0.50/0.47(1)
P	12b	0.6315(5)	0.4599(4)	0.2725(5)	0.3(1)	1
O(1)	12b	0.6508(5)	0.4944(6)	0.4214(8)	1.4(1)	1
O(2)	12b	0.7594(5)	0.4778(4)	0.1881(4)	1.4(1)	1
O(3)	12b	0.5763(4)	0.3166(5)	0.2625(6)	1.4(1)	1
O(4)	12b	0.5231(5)	0.5450(8)	0.2028(4)	1.4(1)	1

Table 2: Results of the Rietveld refinement of $K_2SnIn(PO_4)_3$.

K2SnIn(PO4)3						
Space group, $P2_13$; [Z = 4, a = 10.0460(1) Å; V = 1014(1) Å^3]						
Pseudo-voigt function, PV = ηL + (1-η)G; η = 0.566(1)						
Half-width parameters, U = 0.160(3), V= -0.045(4), and W = 0.015(1)						
Conventional Rietveld R-factors, R_{WP} = 8.1 %; R_P = 6.6 %; R_B = 5.1 %; R_F = 4.0 %						
Atom	Site	Wyckoff positions			B_{iso}(Å^2)	Occupancy
K(1)	4a	0.0696(7)	0.0696(7)	0.0696(7)	2.0(1)	1
K(2)	4a	0.2928(5)	0.2928(5)	0.2928(5)	2.0(1)	1
M(1) = Sn(1)/In(1)	4a	0.5823(2)	0.5823(2)	0.5823(2)	0.9(1)	1
M(2) = Sn(2)/In(2)	4a	0.8494 (2)	0.8494(2)	0.8494(2)	0.9(1)	1
P	12b	0.6221(2)	0.4624(2)	0.2675(2)	0.5(1)	1
O(1)	12b	0.6513(5)	0.5043(6)	0.4098(3)	1.6(1)	1
O(2)	12b	0.7487(5)	0.4896(4)	0.1889(4)	1.6(1)	1
O(3)	12b	0.5673(4)	0.3221(3)	0.2533(6)	1.6(1)	1
O(4)	12b	0.5116(5)	0.5414(6)	0.2005(4)	1.6(1)	1

(a)   **(b)**
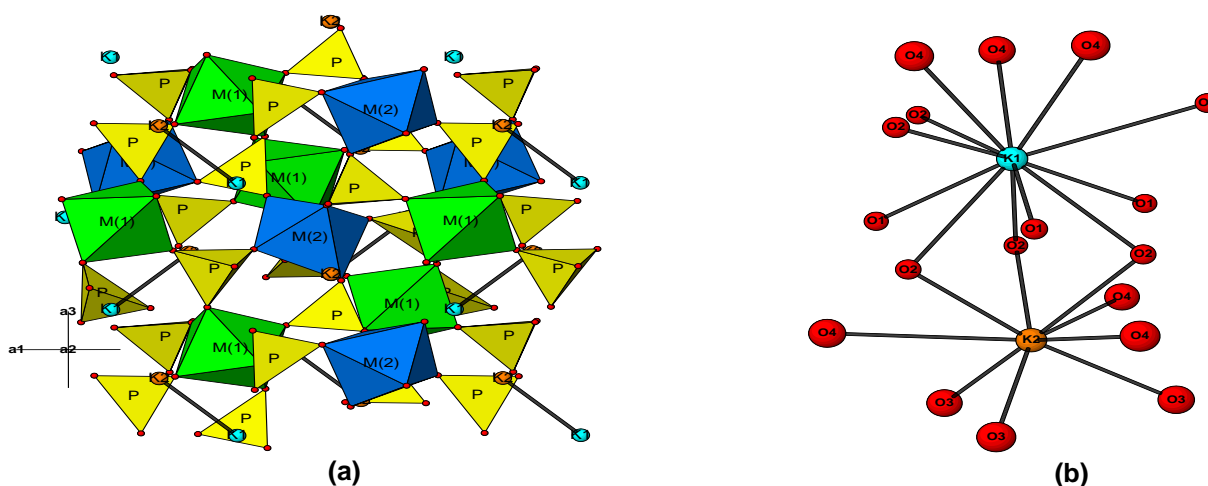
Figure 2: MO_6 and PO_4 polyhedra view in (a) and $K(1)O_{12}$ and $K(2)O_9$ coordination in (b) of $K_2M_2(PO_4)_3$(M = Sn/Cr, Sn/In) Langbeinite framework. The two neighbouring enclosed K(1) and K(2) cations are connected in (a).

A careful analysis of the interatomic distance values shows a high dependence between the Sn/X distribution and the average <M-O> distance values (Table 3). In fact, in $K_2SnCr(PO_4)_3$, the average of <M(1)-O> and <M(2)-O> distance values are 1.95(1) Å and 2.02(1) Å respectively whereas in $K_2SnIn(PO_4)_3$, the same distance are a values of 2.08(1) Å and 2.09(1) Å respectively.

Table 3: Selected interatomic distances (Å) for $K_2[SnX]_M(PO_4)_3$ (X = Cr, In) phases.

	$K_2[SnCr]_M(PO_4)_3$	$K_2[SnIn]_M(PO_4)_3$
P-O distances (Å)		
P-O(1)	1.522(4)	1.510(4)
P-O(2)	1.523(3)	1.521(3)
P-O(3)	1.519(4)	1.520(4)
P-O(4)	1.525(4)	1.522(4)
Average <P-O>	1.52(1)	1.52(1)
K(1)-O distances (Å)		
3×K(1)-O(1)	2.884(2)	2.888(4)
3×K(1)-O(2)	3.097(4)	3.140(3)
3×K(1)-O(2)	3.184(3)	3.214(4)
3×K(1)-O(4)	2.909(4)	2.991(3)
Average <K(1)-O>	3.02(1)	3.06(1)
K(2)-O distances (Å)		
3×K(2)-O(2)	3.150(4)	3.079(4)
3×K(2)-O(3)	2.831(3)	2.801(4)
3×K(2)-O(4)	3.047(3)	3.200(3)
Average <K(2)-O>	3.00(1)	3.03(1)
M-O distances (Å)		
M(1)-O(1)	1.967(4)	2.032(3)
M(1)-O(2)	1.933(3)	2.133(4)
Average <M(1)-O>	1.95(1)	2.08(1)
M(2)-O(3)	2.024(3)	2.145 (3)
M(2)-O(4)	2.032(4)	2.027(4)
Average <M(2)-O>	2.02(1)	2.09(1)

(a) **(b)** **(c)**
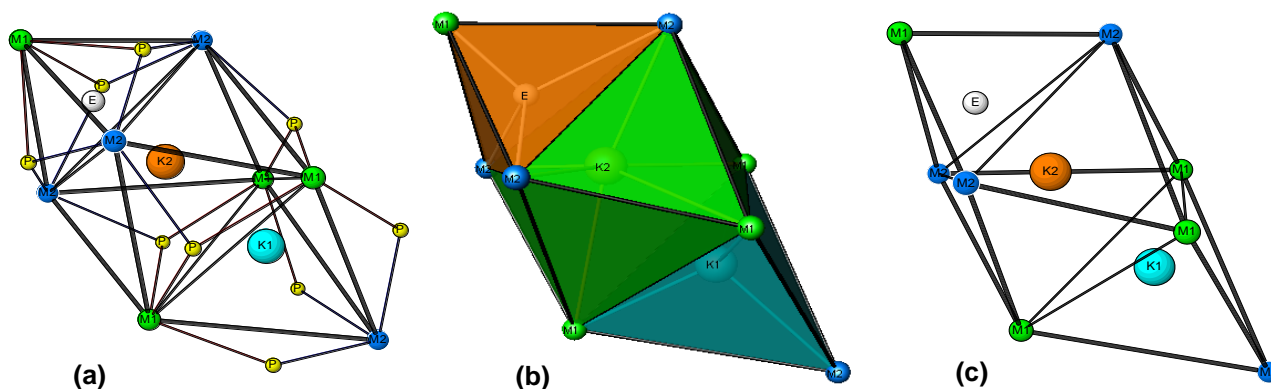
Figure 3: The cages formed around K(1) and K(2) by the M and P atoms (M = Sn/Cr, Sn/In) in $K_2M_2(PO_4)_3$. E is a third possible cationic site within the cage. The P atoms (in yellow) are omitted in (b) and (c).

In both materials the average <M-O> distance values are comparable to the predicted M-O distance calculated from Shannon's table [22]. P-O distance values are comparable to those generally found in phosphate like phases. Within the Langbeinite frameworks, large isolated cages are formed. $K^+(1)$ and $K^+(2)$ cations are best described respectively as twelve and nine-coordinate (Figure 2b). The average <K(1)-O> and <K(2)-O> distance values are (3.02(1) and 3.00(1) Å) for $K_2SnCr(PO_4)_3$ and (3.06(1) and 3.03(1) Å) for $K_2SnIn(PO_4)_3$ respectively. These values show that the cage volume, in $K_2SnIn(PO_4)_3$ is relatively larger than the corresponding one in $K_2SnCr(PO_4)_3$. By considering only the concerned oxygen's, M = (Sb/X) and phosphorus atoms, an improved visualisation of the cages formed in Langbeinite phases, based on $(M_1)_4(M_2)_4P_9O_{48}$ units, are presented in Figure 3a. In fact, each cage contains two K^+ ions separated by 3.86(1) Å and 3.88 (1) Å in $K_2SnCr(PO_4)_3$ and $K_2SnIn(PO_4)_3$, respectively. The two enclosed K atom types are located at each end of the cage. As shown in Figures 3b and 3c, a careful structural analysis of the langbeinite framework shows clearly the presence of a tetrahedral $[E(M_1)(M_2)_3]$ cavity, located opposite the $[K(1)(M_2)(M_1)_3]$ tetrahedra and shares one triangular face with $[K(2)(M_1)_3(M_2)_3]$ octahedra. The empty (E) probable cationic site can accommodate a small cation. To our knowledge, there is no example of a langbeinite structure in which this third possible position is occupied but it should be noted that a similar observation was already signalised for other

langbeinites [17,23]. X-ray powder diffraction data, obtained from the ''observed and calculated intensities'' of the Rietveld refinement (Cu$K\alpha1$: 1.540 56 Å), for both $K_2SnX(PO_4)_3$ (X = Cr, In) materials are given in Table 4 and Table 5 respectively.

Table 4: Powder diffraction data of $K_2SnCr(PO_4)_3$ (Cu$K\alpha_1$; λ = 1.54056 Å).

hkl	$d_{obs.}$(Å)	100 I/I_0 (obs.)	100 I/I_0 (cal.)	hkl	$d_{obs.}$(Å)	100 I/I_0 (obs.)	100 I/I_0 (cal.)
111	5.7008	36	37	440	1.7455	2	1
120	4.4158	52	49	441	1.7188	8	7
211	4.0311	22	23	350	1.6934	3	3
220	3.4910	1	1	160	1.6233	3	3
221	3.2913	9	9	352	1.6018	14	12
130	3.1224	100	100	260	1.5612	2	2
311	2.9771	27	28	261	1.5421	4	4
222	2.8504	1	1	451	1.5236	1	1
230	2.7386	11	10	622	1.4886	2	1
231	2.6390	70	70	360	1.4719	5	5
400	2.4685	1	1	361	1.4558	6	5
140	2.3948	3	3	444	1.4252	1	1
330	2.3273	1	1	362	1.4106	3	2
331	2.2653	2	2	170	1.3964	3	3
240	2.2079	1	1	551	1.3826	1	1
241	2.1547	3	3	270	1.3563	2	2
332	2.1052	2	2	544	1.3078	1	1
422	2.0155	14	14	370	1.2965	1	1
340	1.9748	5	5	371	1.2855	2	2
150	1.9365	11	11	471	1.2154	1	1
333	1.9003	5	5	733	1.2063	1	1
250	1.8336	13	13				
251	1.8027	3	3				

Table 5: Powder diffraction data of $K_2SnIn(PO_4)_3$ (Cu$K\alpha_1$; λ = 1.54056 Å).

hkl	$d_{obs.}$(Å)	100 I/I_0 (obs.)	100 I/I_0 (cal.)	hkl	$d_{obs.}$(Å)	100 I/I_0 (obs.)	100 I/I_0 (cal.)
111	5.8001	44	41	352	1.6297	12	12
120	4.4927	70	66	260	1.5884	4	2
211	4.1013	35	32	261	1.5689	5	4
220	3.5518	1	1	451	1.5501	4	4
221	3.3487	14	14	622	1.5145	1	1
130	3.1768	100	100	360	1.4976	5	4
311	3.0290	24	23	361	1.4812	4	4
230	2.7863	11	10	444	1.4500	1	1
231	2.6849	72	74	362	1.4351	3	2
400	2.5115	1	1	170	1.4207	3	3
140	2.4365	4	4	551	1.4067	2	2
330	2.3679	1	1	270	1.3799	2	2
331	2.3047	3	3	271	1.3671	1	1
241	2.1922	4	4	462	1.3425	1	1
332	2.1418	1	1	544	1.3306	1	1
422	2.0506	18	17	370	1.3191	1	1
340	2.0092	6	5	371	1.3079	2	2
150	1.9702	16	14	372	1.2758	1	1
333	1.9334	6	6	180	1.2461	2	2
250	1.8655	15	14	471	1.2366	1	1
251	1.8341	2	1	660	1.1839	3	2
440	1.7759	1	1	381	1.1678	2	1
441	1.7488	7	7	555	1.1600	1	1
350	1.7229	4	3	382	1.1449	1	1
160	1.6516	2	2				

Conclusions

Structures of the two $K_2SnX(PO_4)_3$ (X= Cr, In) Langbeinite phases were determined by XRD technique using the Rietveld analysis. The framework is built of $Sn(X)O_6$ octahedra sharing corners with PO_4 tetrahedra. In contrast to the Nasicon phases where interconnected interstitial sites through which one-valent cations can diffuse exist, in the Langbeinite framework the channels between the holes have narrow windows and only isolated large cages containing a maximum of two K atoms are considered. Note that the Langbeinite structure is generally favoured when the A cation in $A_2M_2(PO_4)_3$ is larger than 1 Å (e.g.; K^+, Rb^+, Cs^+, Ba^{2+}, Pb^{2+}). So cations of a sufficiently large size remain captive in the cages and lose their ability to migrate. This characteristic may be useful in developing materials for the immobilisation of toxic cations (i.e. $^{137}Cs^+$) from wastes, including radioactive waste [24]. It is important to note that during this careful structural analysis we have shown the possibility of a third new empty cationic site (labeled E) which can accommodate a small cation such as Li^+.

References

1. Hagman L., Kierkegaard P., *Acta Chem. Scand*. 22 (1968) 1822.
2. Masse R., Durif A., Guitel J-C., Tordjman I., *Bull. Soc. Fr. Mineral Crystallogr*. 95 (1972) 47.
3. Zah-Letho J. J., Verbaere A., Jouanneaux A., Taulelle F., Piffard Y., Tournoux M., *J. Solid State Chem*. 116 (1995) 335.
4. Ogorodnyk I. V., Zatovsky I. V., Slobodyanik N. S., Baumer V. N., Shishkin O. V., *J. Solid State Chem.* 179 (2006) 3461.
5. Nikolay Slobodyanik S., Kateryna Terebilenko V., Ivan Ogorodnyk V., Igor Zatovsky V., Maksym Seredyuk, Vyacheslav Baumer N., Philipp Gütlich, *Inorg. Chem.* 51 (2012) 1380.
6. Zhang Z. J., Lin X., Zhao J. T., Zhang G. B., *Mater. Res. Bull*. 48 (2013) 224.
7. Chawla S., Ravishanker, Rajkumar, Khan A. F., Kotnala R. K., *J. Lumin*.136 (2013) 328.
8. Hikita T., Sato S., Sekiguchi H., Ikeda T., *J. Phys. Soc. Jpn*. 42 (1977) 1656.
9. Sathasivam P. K., Buvaneswari G., *J. Alloys Compd*. 615 (2014) 419.
10. Orlova A.I., Orlova V.A., Orlova M.P., Bykov D.M., Stefanovskii S.V., Stefanovskaya O.I., Nikonov B.S., *Radiochemistry* 48 (2006) 330.
11. Battle P.D., Cheetham A.K., Harrison W.T.A., Long G.J., *J. Solid State Chem*. 62 (1986)16.
12. Norberg S. T., *Acta Crystallogr*. *Sect.B: Struct. Sci.* B58 (2002) 743.
13. Shpanchenko R.V., Lapshina O.A., Antipov E.V., Hadermann J., Kaul E. E., Geibbel C., *Mater. Res. Bull*. 40 (2005) 1569.
14. Aatiq A., *Powder diffr.* 19 (2004) 272.
15. Antony C.J., Aatiq A., Panicker C.Y., Bushiri M.J., Varghese H.T., Manojkumar T.K., *Spectrochim. Acta, Part A* 78 (2011) 415.
16. Aatiq A., Haggouch B., Tigha R., *Global J. Phys. Chem.* 2 (2011) 129.
17. Aatiq A., Haggouch B., Bakri R., Lakhdar Y., Saadoune I., *Powder Diffr*. 21(2006) 214.
18. Hai-Yan Li, Dan Zhao, *Acta Crystallogr. Sect.E: . Struct. Rep.* E67 (2011) i56.
19. Harrison W. T. A., *Acta Crystallogr.Sect.C: Cryst. Struct.Commun.* C66 (2010) i82.
20. Rodriguez-Carvajal J., *Phys. Rev. B: Condens. Matter.* 192 (1993) 55.
21. Boultif A., Louër D., *J. Appl. Crystallogr*. 37 (2004) 724.
22. Shannon R. D., *Acta Crystallogr., Sect. A: Cryst. Phys., Diffr., Theor. Gen. Crystallogr.* A32 (1976) 751.
23. Gustafsson J. C. M., Norberg S. T., Svensson G., Albertsson J., *Acta Crystallogr., Sect. C: Cryst. Struct. Commun*. C61 (2005) i9.
24. Orlova A. I., Orlova V. A., Buchirin A. V., Korchenkin K. K., Beskrovnyi A. I., Demarin V. T., *Radiochemistry* 47 (2005) 235.

(2017) ; http://www.jmaterenvironsci.com